DOI: 10.13009/EUCASS2019-86

Simulation of Inflation Driving Deployment of Rolled Elastic Thin Wall Boom with Velcro Constraints

Jian Gao★, Ping Tang★*, Chao Xie*, Fujun Peng★*, Hua Zhang★**

★Institute of Aerospace System Engineering Shanghai, Shanghai 201108, China
**Shanghai Key Laboratory of Spacecraft Mechanism, Shanghai 201108, China*
3805 Jindu Road, Minhang District, Shanghai, China
Corresponding author: Jian Gao, E-mail: hanggaojian@163.com

Abstract
The flexible deployment structure has played an increasingly important role in space missions such as manned spaceflight, deep space exploration, due to its light weight and high storage ratio. In this study, we present a simple flexible deployment structure, which contains CFRP (carbon fibre reinforced plastic) boom, airbag and Velcro. We introduce the Velcro to constrain the coiled boom and the airbag to drive the deployment. Inflation process of tubular airbag is simulated to get the structural stress characteristics of the structure. The peeling process of Velcro is also simulated and a good comparation with the peeling experiments results is presented. Based on the analysis of Velcro and airbag, A complex finite element model of this structure is built to simulate the deployment process of the coiled boom constrained by Velcro.

1. Introduction

The CFRP (carbon fibre reinforced plastic) boom with lenticular section can be flexible when it is squashed, but it has high stiffness when the section is fixed.[1,2,3] The best way to collection the boom is to roll it up, but without the proper constraints, the curled boom will automatically unfold. To solve this problem, we introduce the Velcro to constrain it. This paper chooses the airbag and Velcro to control the deployment of CFRP boom which is coiled on a roller. A complex finite model is built to simulate the deployment of CFRP boom which is coiled on a roller, restrained by Velcro and driven by airbag.

Airbag and Velcro are used as the driving source and constraints of coiled thin-wall boom. The process of the Velcro peeling and the inflatable deployment of the coiled thin-wall boom which is constrained by Velcro are analyzed by numerical simulation.[4,5,7]

The finite element model of peeling process of Velcro with hooks and loops is built based on the cohesive zone model of fracture mechanics.[6] By changing the peeling angle of Velcro, the laws of peeling force's changing are obtained. Some peeling experiments of Velcro are carrying out and the results are compared.

Based on the theory of surface-based fluid modelling method, the finite element model of airbag is built. By changing the mass flow rate, the structure stress states of inflatable airbag are obtained.

The finite element model of elastic thin-wall boom (CFRP boom) is built with material of carbon fibre composite. Considering Velcro constraining and airbag driving, the finite element model of coiled boom is built by pulling and rolling process in ABAQUS. The process of inflatable deployment of this boom is simulated and its dynamics properties are obtained.

Final conclusions, the finite element model in peeling process of Velcro is built which is efficient compared with the way which builds every loop and hook in Velcro. And a good comparison between simulations and experiments is obtained. A complex finite element model is built in which we need to solve some tricky problem including large deformation, complex contact.

2. Design of inflated deployable structure with Velcro constraints

The elastic thin-wall boom is curled and has huge strain energy in it, which makes the boom obtain strong resilience to restore initial shape. However, the thin-wall boom in the curled state is incapable of moving by the flexible

DOI: 10.13009/EUCASS2019-86

hooking on Velcro. In order to realize the controllable deployment of the thin-wall boom, the flexible hook is realized by the driving force in the inflation process of the airbag.

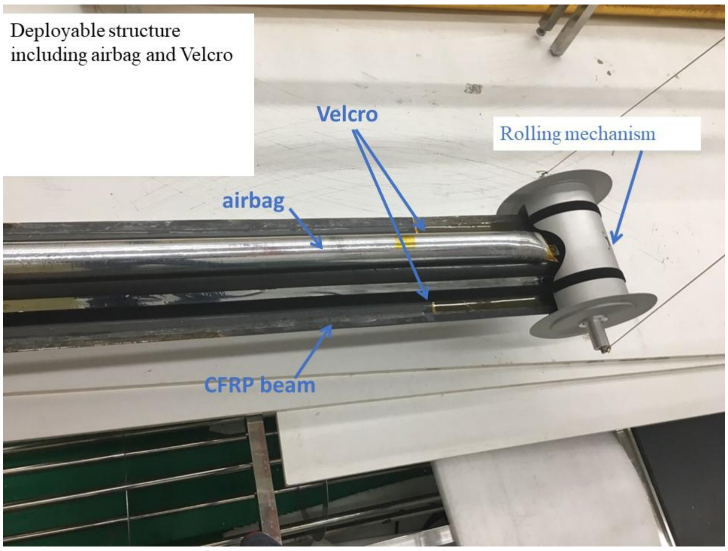

Figure 1: Inflated deployable structure

3. Dynamic analysis of the deploying process

3.1 Finite element simulation of inflation process

3.11 The theory of fluid cavity modelling method

The face-based fluid cavity modelling method is different from the fluid-solid coupling method. This method ignores the inertia in the fluid flow process and the structural effect generated by the fluid flow while introducing the gas mass to calculate pressure. This method is good at simulating the interaction between fluid and structure, especially the state of the inflatable structure in the late stage of inflation.

The modelling method establishes a cavity model with a closed face and a reference point, where the pressure values are equal everywhere at any time. The aeration process is free of heat exchange with the outside world and is an adiabatic process. The absolute pressure of the gas in the cavity during inflation can be expressed as flow.

$$\tilde{p} = p + p_A = \rho R(\theta - \theta^Z) \quad (1)$$

Where the p_A is the ambient pressure, p is the pressure measurement, ρ is the gas density, R is the gas constant, and θ , θ^Z is the current temperature and absolute zero.

According to the first law of thermodynamics, the energy change rate at any time during airbag inflation can be derived:

$$\frac{d(mE)}{dt} = \dot{m}_{in} H_{in} - \dot{m}_{out} H_{out} - \dot{W} - \dot{Q} \quad (2)$$

Where m is the total mass of the gas in the airbag, E is the internal energy of the gas, $\dot{m}_{in}$is the mass flow rate of the charge, H_{in} is the specific enthalphy of the gas in, $\dot{m}_{out}$ is the mass flow rate of the effluent gas, H_{out} is the ratio of the effluent gas, the power of the gas charging, and the airbag Cooling power.

The reference point in the airbag model forms a polyhedron with the four nodes of each unit of the cavity, as shown in Figure 2. When the pressure increases during the inflation process, the coordinates of the four nodes of the unit change, and the volume of the polyhedron is changed at the same time. By calculating the volume change of the polyhedron before and after the movement of each unit, and then adding them, the whole volume change during inflation of the airbag is obtained.

DOI: 10.13009/EUCASS2019-86

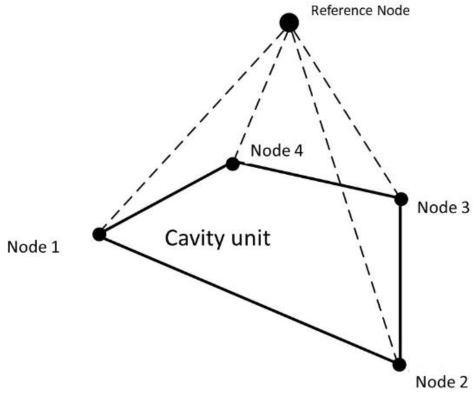

Figure 2: Cavity unit and nodes

3.1.2 Simuation of inflated tubular airbag

This chapter carries out simulation analysis on inflation process the tubular airbag with a diameter of 100mm. Based on the face-based fluid cavity modelling method, the finite element model of the tubular airbag is established. On this basis, the aeration process of the straight airbag under proper inflation flow conditions is firstly analyzed, and the stress change of the airbag wall structure during the deployment process is obtained.

The finite element model of the tubular airbag is established in the finite element analysis software ABAQUS, and is composed of a cavity body, a reference point. The tubular airbag has a transverse diameter of 10 cm, a thickness of 10μm, and a longitudinal length of 3 m. The model is divided by the general 4-node quadrilateral reduced-integration shell element S4R. This type of element reduces the integral points in each direction compared with the ordinary complete integration element, and the performance is stable. It is more suitable for finite element simulation of large deformation structures such as flexible airbags. Analysis, the finite element model of the airbag is shown in Figure 3.

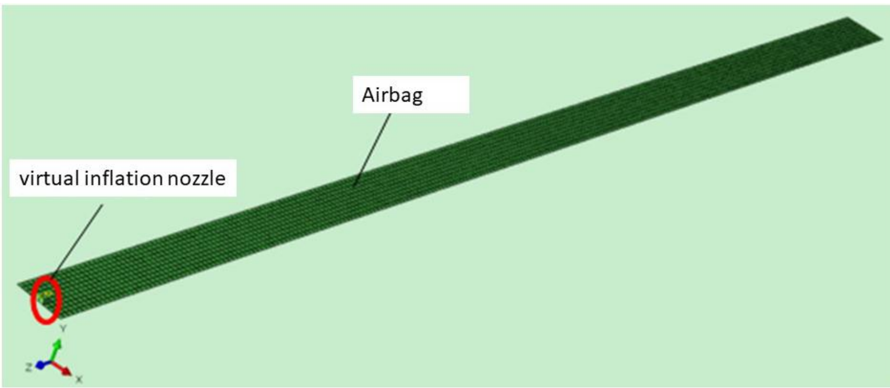

Figure 3: FE model of airbag

In the finite element model, the element side length is 10mm, and the whole model consists of 50110 S4R elements. Regardless of material nonlinearity, the airbag structure density is 1600 kg/m^3, the Young's modulus is 1300 MPa, and the Poisson's ratio is 0.3. Detailed geometry and material parameters are shown in Table 1.

Table 1: Finite element model parameters

geometric parameters	length	diameter	thickness
	3m	10cm	10μm
material parameters	density	Young's modulus (E)	Poisson's ratio (υ)
	1600kg/m^3	1300MPa	0.3
element parameters	type	size	number
	S4R	3mm*4mm	50110

DOI: 10.13009/EUCASS2019-86

The face-based fluid cavity modelling method requires that the cavity must be completely closed in order to correctly calculate the volume change of the cavity during simulation, otherwise the simulation cannot be performed normally. To establish a cavity model in ABAQUS, we must first define a unique cavity reference point. In addition, we need to define the initial shape of the airbag. After the pre-processing module establishes the geometric model of the airbag, it is necessary to further improve the model. Because the keyword of the *Fluid inflator and its attribute (*Fluid inflator property) parameters in the finite element model of the airbag are not supported in GUI of ABAQUS pre-processing module, it needs to be manually written in the inp file generated by the pre-processing module. Enter keywords such as air pump. After modifying the parameters such as inflation mode, air pressure, and air flow in the inp file, the modified inp file is submitted to the ABAQUS solver for calculation.

By comparing the pressure and volume changes during the inflation process. The stress characteristics of the airbag during the inflation process are shown in Figure 4.

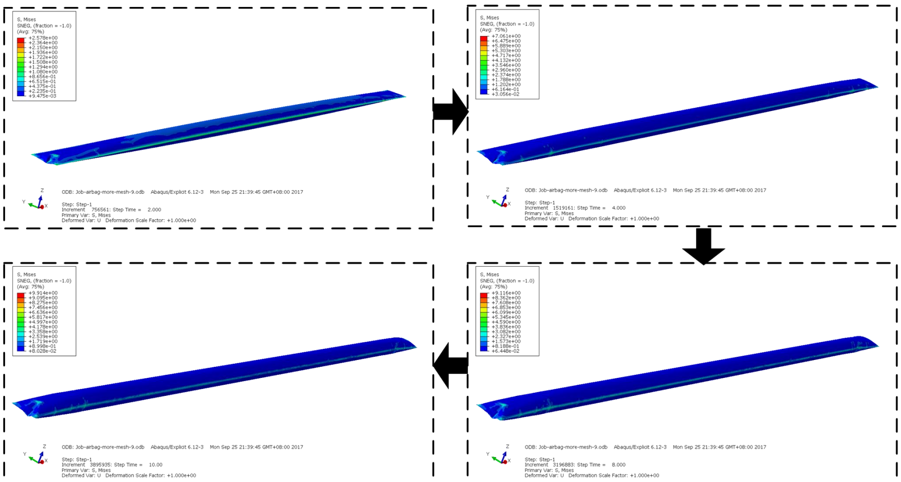

Figure 4: Airbag inflation process with flow rate 0.36g/h

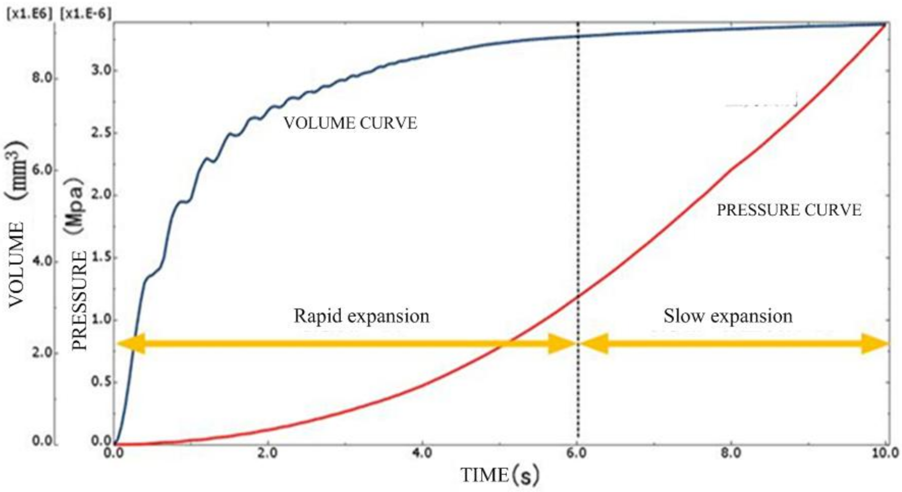

Figure 5: Airbag volume and pressure curves

It can be seen from Figures 5 that as the volume of the cavity increases, the pressure increases slowly during this process. When the volume reaches a certain range, the inflation continues, and the pressure continues to increase, but the volume change is small. At this time, the wall of the tube becomes harder and harder as the pressure in the inner chamber increases.

During the inflation process of the airbag, as the internal pressure increases, the tensile stress on the airbag wall increases continuously. When the maximum tensile strength of the material of the airbag wall exceeds, the airbag will be destroyed.

From the stress cloud diagrams of the airbags in Figure 6 , it is known that during the inflation process, the areas with greater stress are mainly distributed in the middle and both ends of the airbag. The inflation flow rate is 3.6kg/h and the inflation time is 10s. The maximum stress of the airbag structure is 36.37MPa. The tensile strength of the

DOI: 10.13009/EUCASS2019-86

aluminized PET polyester film is about 200 MPa, which can fully withstand the air pressure during the inflation process.

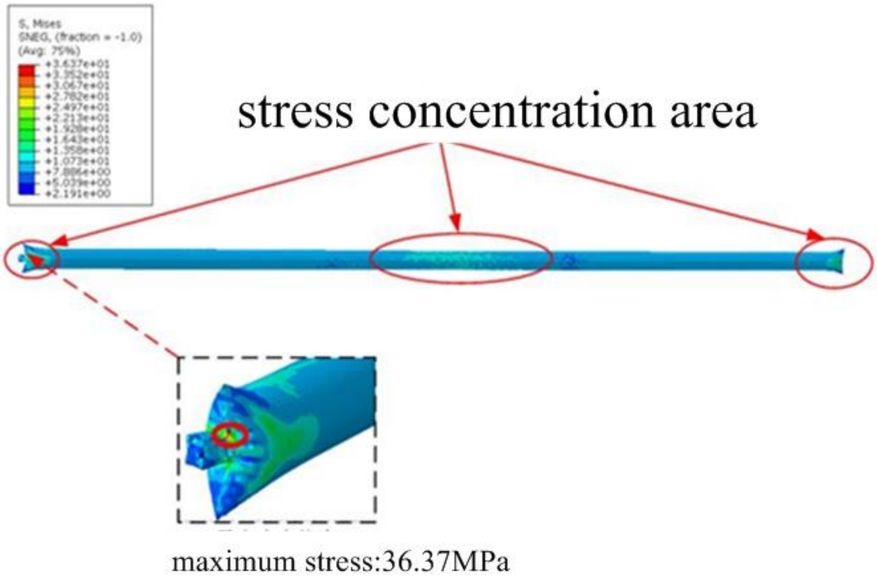

Figure 6: Stress distribution of airbag

3.2 Simulation of Velcro's peeling process

3.2.1 Cohesive zone model

The Velcro has a complicated action form between the hook and loop during the peeling process, and a hook type structure may hook several loops at the same time, and the number of the hook loops is accidental. If the stress failure method is still used to study the Velcro peeling failure process, it will cause a large error in the analysis results and huge amount of calculation. The dynamic mechanical model of the Velcro's peeling process is established by the bilinear tension displacement method in the elastoplastic fracture mechanics CZM method. [7]

The concept of cohesive zone was first introduced by Dugdale in the study of crack propagation in fracture mechanics. He found that when the sheet with initial damage is stretched, the plastic zone near the crack tip is flat, which coincides with the cohesive force to counteract the tensile force at the crack. Subsequently, Barenbatt officially proposed CZM in 1962, and successfully solved the stress singularity problem at the crack tip in linear elastic fracture mechanics by using CZM. The distribution of the cohesive zone are shown in Figure 7.

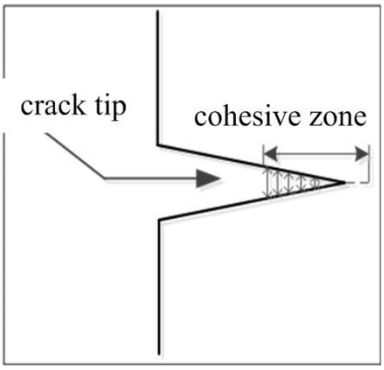

Figure 7: The distribution of the cohesive zone

In the process of peeling of the Velcro, the combination of hook and loop is continuously invalid, and at the same time a new combination of hooks acts. CZM generates a new texture interface while simulating crack propagation,

DOI: 10.13009/EUCASS2019-86

which is similar to the action mode of the hooking action zone in the peeling process of the Velcro. At the same time, by defining the evolution law of crack damage in CZM, it can also describe that the Velcro is stripped.
The key of simulation using CZM is to define the relationship between tension and displacement, and to set mechanical parameters (extreme stress, fracture energy, etc.). There are many kinds of tension displacement relationships, such as bilinear type and exponential type. In this paper, the bilinear rule is used to simulate the relationship between peeling displacement and stress during the Velcro stripping process, as shown in Figure 8.

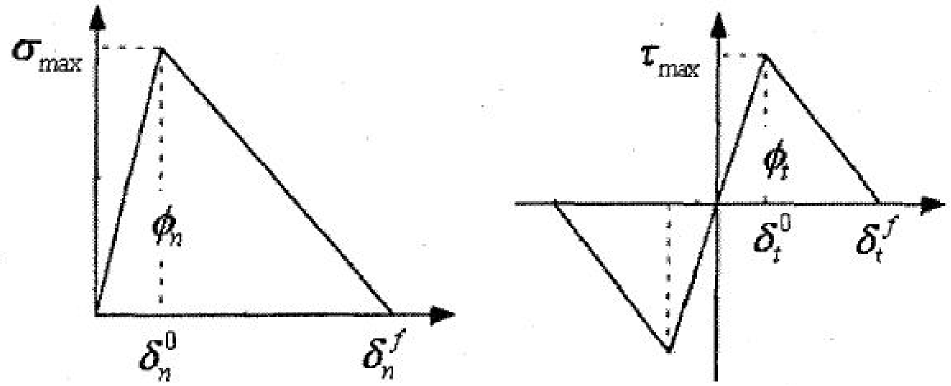

Figure 8: The bilinear rule of CZM

As shown in Fig 8, under the external tension, as the normal displacement of the Velcro action area increases, the normal stress of the hook-and-loop combination also increases, when the hook-and-loop combination is When the tension is pulled, the ultimate stress value is reached, and the hook and loop combination begins to fail. This process can be equivalent to the crack damage expansion phase until the hook-fusing combined stress is reduced to zero, and the combination is completely ineffective. The area enclosed by the tension displacement curve is equivalent to the energy required for the crack. The ultimate stress value of this process depends on the size of the CZM region and the elastic modulus of the material. The relationship between normal and tangential stress displacement in the bilinear tension displacement law can be expressed as:

$$\mathrm{T}_n = \begin{cases} \dfrac{\sigma_{\max}}{\delta_n^0}\delta & (\delta \le \delta_n^0) \\ \sigma_{\max}\dfrac{\delta_n^f - \delta}{\delta_n^f - \delta_n^0} & (\delta > \delta_n^0) \end{cases} \tag{3}$$

$$\mathrm{T}_t = \begin{cases} \dfrac{\tau_{\max}}{\delta_t^0}\delta & (\delta \le \delta_t^0) \\ \tau_{\max}\dfrac{\delta_t^f - \delta}{\delta_t^f - \delta_t^0} & (\delta > \delta_t^0) \end{cases} \tag{4}$$

The equation represents the stress values in both the normal and tangential directions, and the maximum stress values in both directions Where the T_n is the normal stress, σ_{max} is the ultimate stress, and δ_n^f is peeling displacement, δ_n^0 is the peeling displacement when it is ultimate stress. And the variables of tangential peeling are similar to the normal peeling.

3.2.2 Finite element model of Velcro

The finite element model of Velcro is built in ABAQUS software. It consists of three parts: two thin shells simulating the base layer on the upper and lower sides of the Velcro, and the Cohesive unit simulating the area of the hook and loop. The Cohesive unit model has a thickness of 3 mm and a width of 15 mm, which is consistent with the thickness of the Velcro in actual working conditions. The finite element model and physical object of the Velcro are shown in Figure 9.

DOI: 10.13009/EUCASS2019-86

Figure 9: The FE model and physical object of Velcro

The Velcro has a lateral width of 15 mm, a longitudinal length of 200 mm, and a bonding thickness of 3 mm. The solid model of the cohesive layer and the upper and lower base layers are respectively established in ABAQUS. The detailed model section is shown in Figure 10, in which the base layer is constructed in the form of a thin shell. Finally, the binding constraint is used to fix the central cohesive layer and the base layer to ensure the displacement and stress coordination of the elements on both sides of the Velcro.

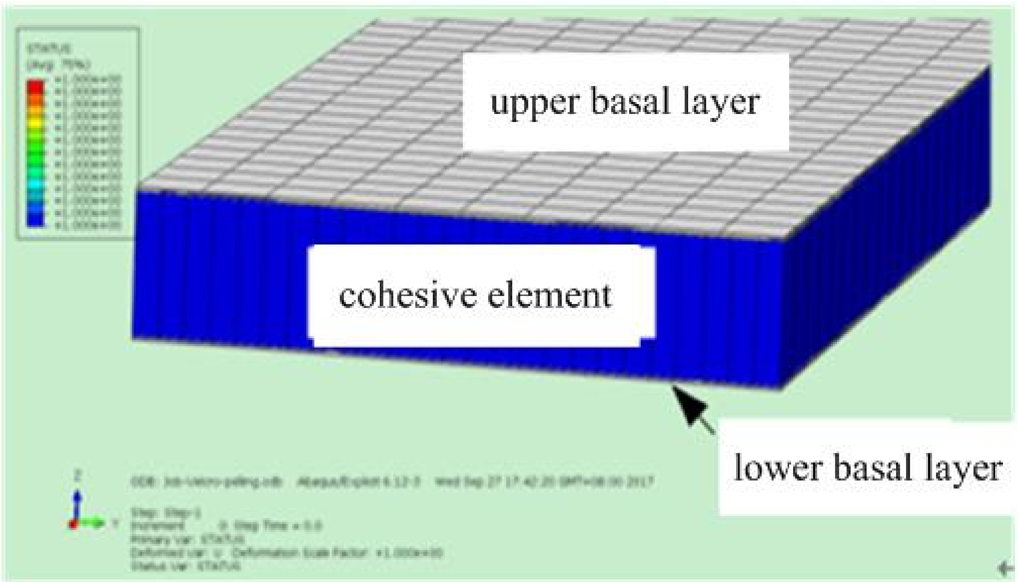

Figure 10: The detailed model section of Velcro

3.2.3 Simulation of Velcro peeling process

During the peeling process of the Velcro, the angle between the upper base surface and the horizontal line is the angle of the buckle peeling (the peeling angel is shown in Fig 11). The hook-and-loop model was 1 m long, and when the peeling speed was 50 mm/s, the peeling angle was set to 30°, 45°, 60°, 70°, 80°, and 85°. On this basis, the simulation results of the Velcro peeling force under different peeling angles were analyzed, and the influence of the change of the peeling angle on the peeling force was obtained. The results are shown in Fig 12.

DOI: 10.13009/EUCASS2019-86

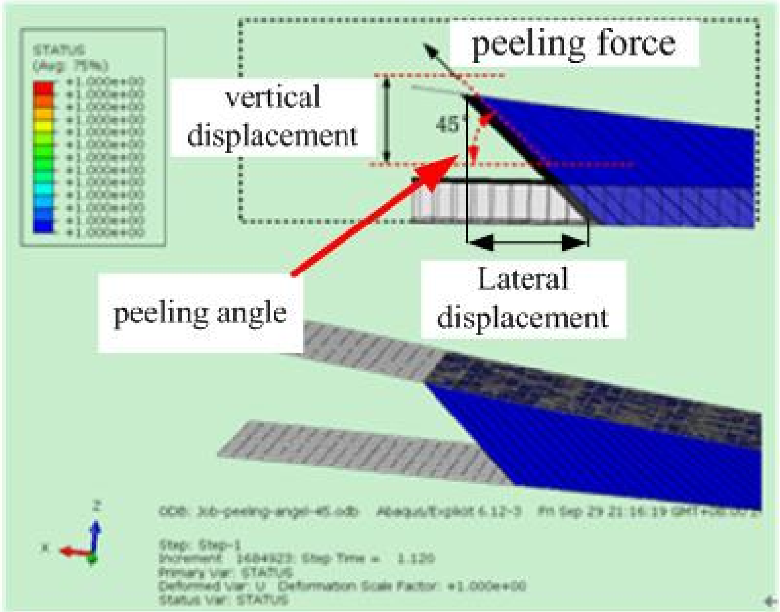

Figure 11: The peeling angle in the model

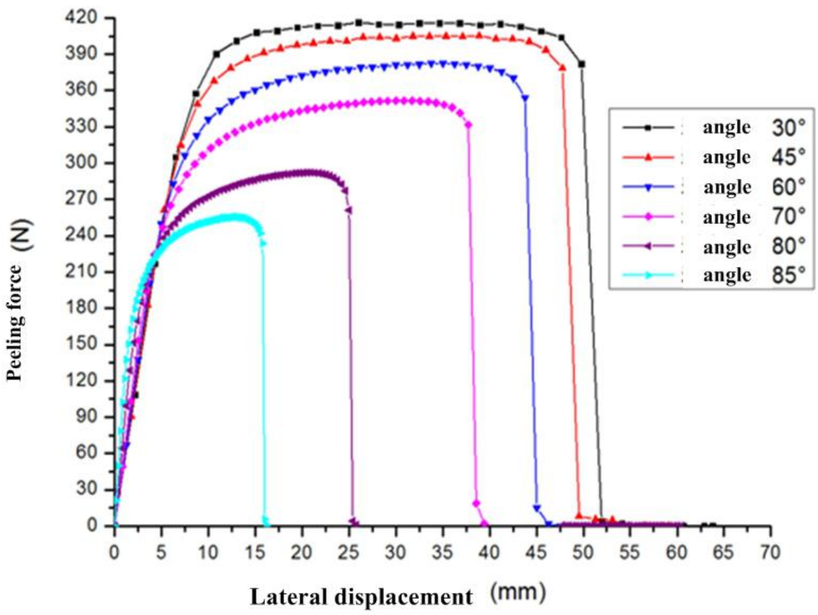

Figure 12: The peeling force curves with different peeling angles

Figure 12 shows the peel force versus displacement for different peel angles. It can be seen from the curves that as the peeling displacement increases, the peeling force rapidly increases from 0 to the maximum value, and rapidly decreases to 0 after the stable peeling section. The results of comprehensive simulation calculations can be concluded that the change of the peeling angle has a great influence on the peeling force. As the angle increases, the peeling force of the stable peeling section decreases.

3.2.4 Experiments of Velcro peeling process

The Velcro undergoes a process of hooking each other during the peeling process, which is stretched until it is slipped. In this process, the action form of the hook and loop combination is more complicated, mainly reflected in the randomness of the number and position of the hook and the loop. In order to obtain the mechanical properties of

DOI: 10.13009/EUCASS2019-86

the Velcro during the peeling process, the experimental verification under 180° peeling conditions was carried out. It has been verified that the variation of the peel force fluctuation in the simulation and the experiment is basically the same.

Figure 13: The testing machine : UTM4000

The finite element software ABAQUS was used to establish a simulation model under the 180° peeling condition of the flexible hook. The peeling speed was set to 60 mm/min. The simulation model is shown in the figure14, and the peeling force changes as shown in .

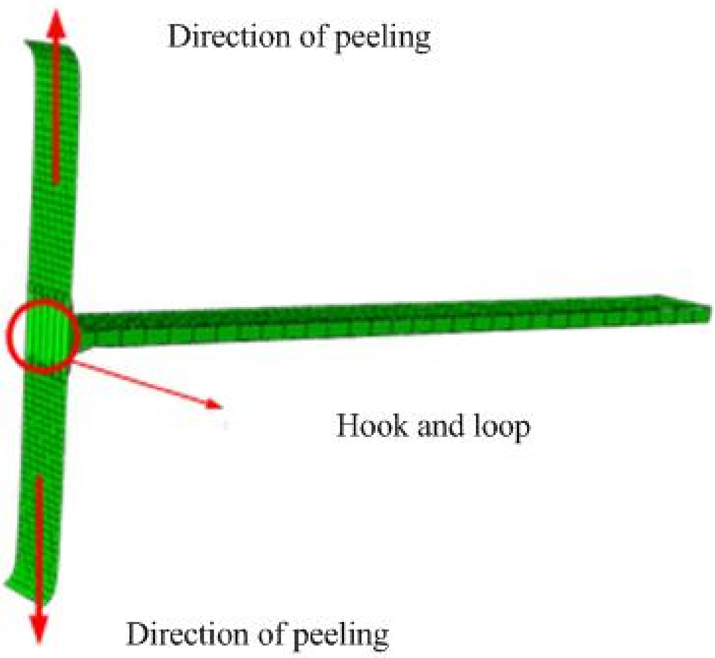

Figure 14: The simulation model with peelig angle 180°

DOI: 10.13009/EUCASS2019-86

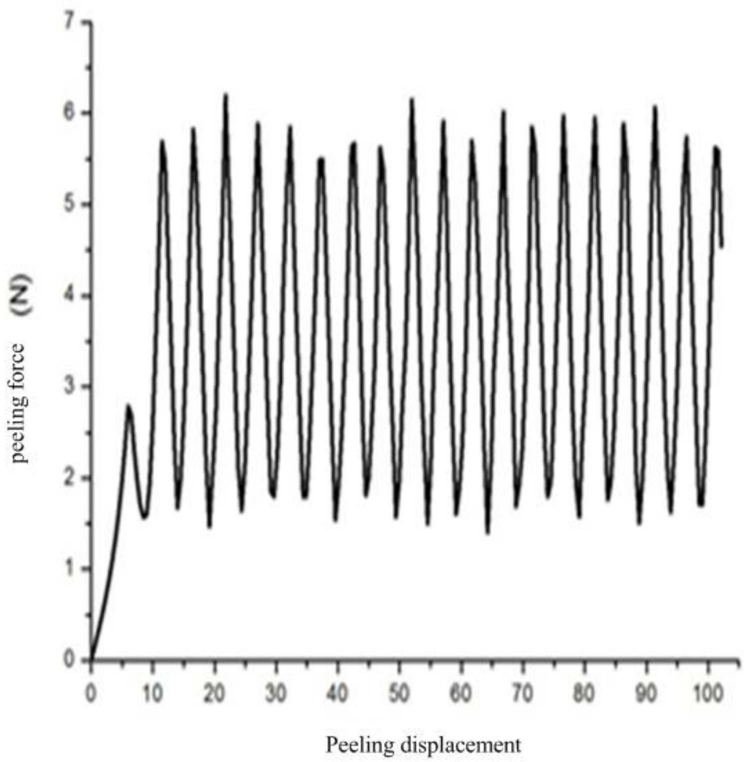

Figure 15: The curve of peeling force in simulation

The Velcro specimen used in the peeling test was 20 cm in length and 15 mm in width. Before the start of the peeling test, in order to fully bond the hook surface and the matte side of the hook, the Velcro was continuously pressed for 5 minutes with a weight of 5 kg which I shown in Fig 16.

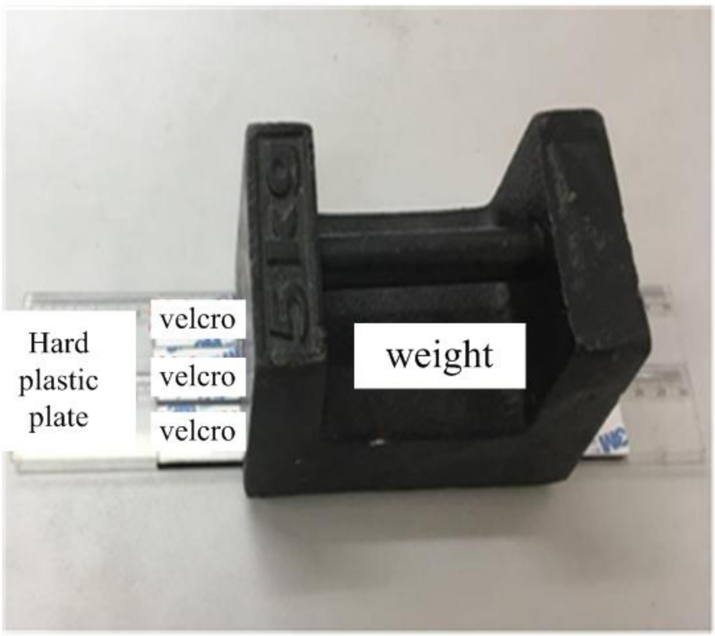

Figure 16: Compacting the Velcro

In the initial state of the experiment, the hook surface and the matte side of the hook test piece were respectively clamped on the upper and lower clamps of the tensile tester. In order to make the measurement result more accurate, the range of the experimental machine sensor is 50N, the stretching speed is set to 60mm/min, and the Velcro stripping process is shown in Figure 17.

DOI: 10.13009/EUCASS2019-86

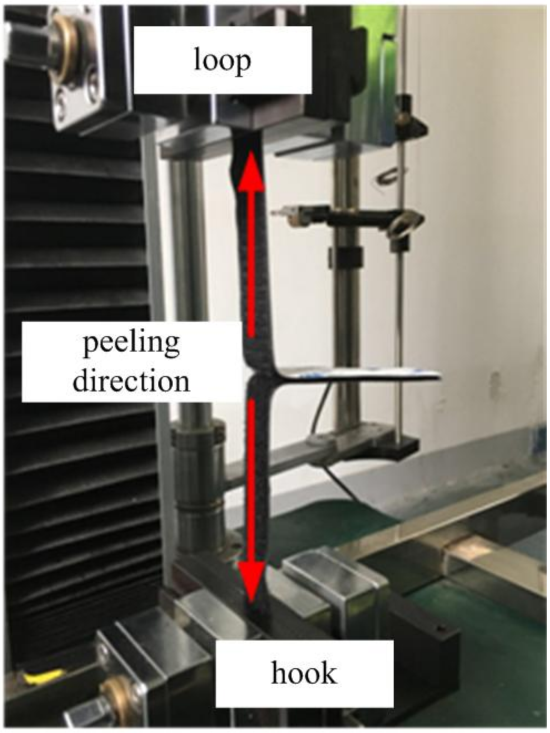

Figure 17: The peeling experiments of Velcro with 180 °

Comparing the measured curve with the mean curve, the fluctuation of the mean curve is obviously weakened, which can well describe the change of the peel force of the flexible hook. Comparing the experimental mean curve with the simulation result curve, the simulation results agree well with the experimental results, as shown in Figure 18.

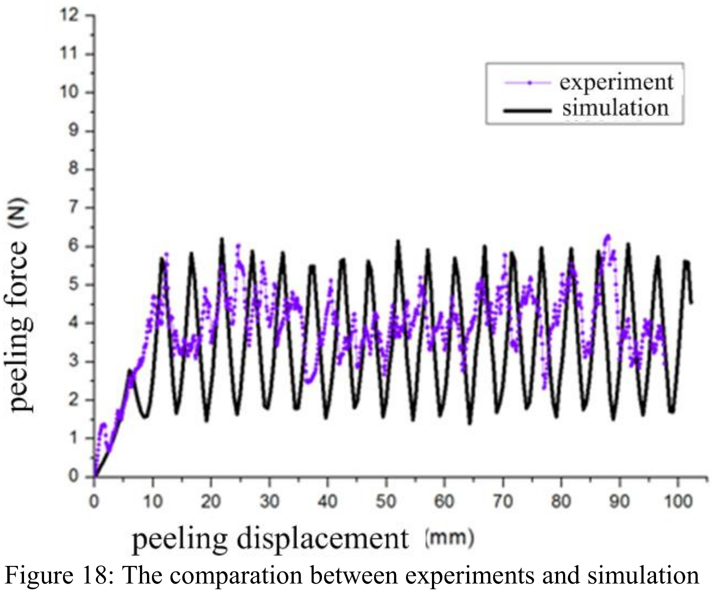

Figure 18: The comparation between experiments and simulation

3.3 Simulation of inflated deployment process

This chapter establishes a finite element model of elastic thin-wall boom with flexible constraints. By inflating the airbag, the thin-wall boom are deployed controllably. The process of the unfolding motion (the motion of the centre point of the roller) is analyzed.

DOI: 10.13009/EUCASS2019-86

3.3.1 FE model of CFRP beam

The cross-sectional shape of the elastic thin-wall boom is pod-shaped, and the object is designed by composite paving. The finite element model is based on the shell and is meshed by S4. The finite element model of the boom and the section dimensions are shown in Figure19.

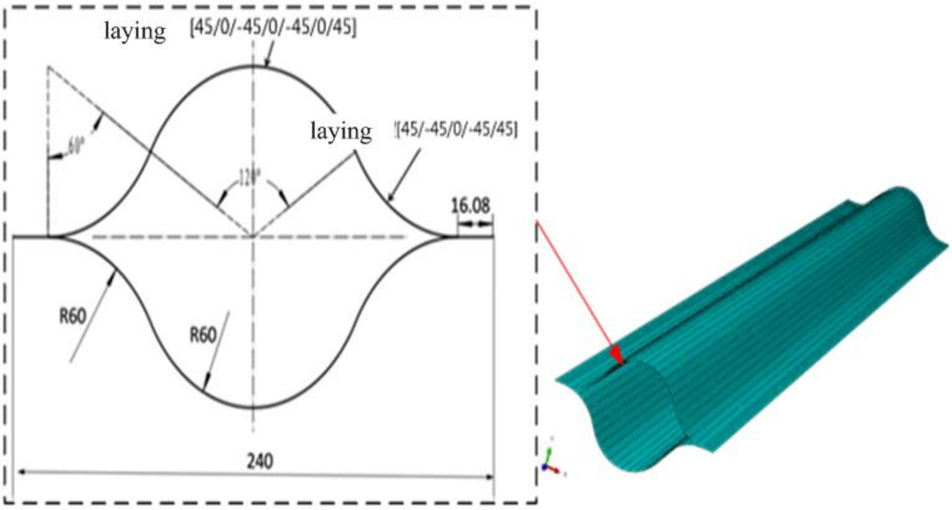

Figure 19: The finite element model of the boom

The finite element model of the elastic thin-wall boom has a longitudinal length of 3 m and a single layer thickness of 0.04 mm. The specific finite element model geometry and material parameters are shown in Table 2. The fibre wall laminate of the boom wall composite is shown in Figure 20.

Table 2: Finite element model geometry and material parameters of boom

single layer material properties	value
density(g/cm^3)	1.6
0°Tensile modulus (GPa)	80
90°Tensile modulus (GPa)	6
Poisson's ratio	0.3
shear modulus (GPa)	2.5

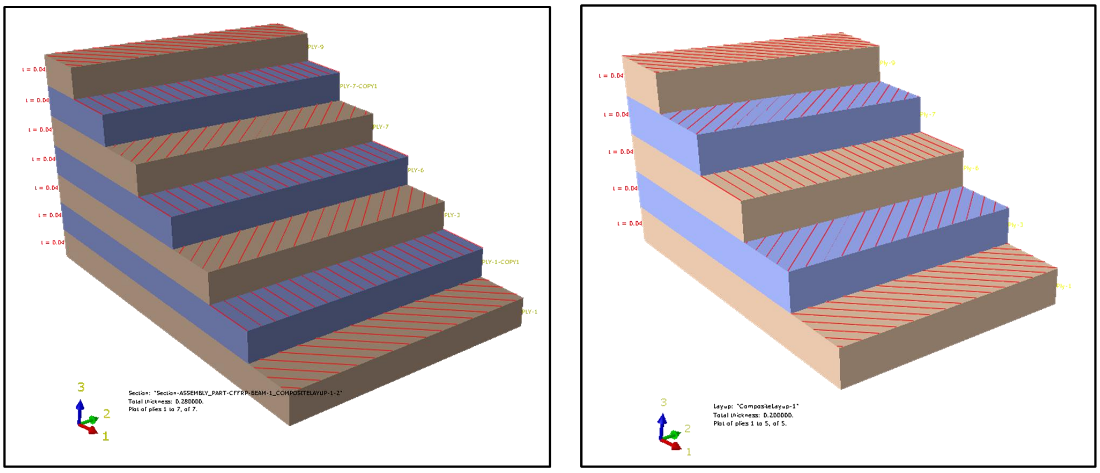

Figure 20: Layers design of the boom

DOI: 10.13009/EUCASS2019-86

3.3.2 FE model of CFRP boom with airbag and Velcro

The finite element model of the inflatable thin-wall boom includes three parts: a pod-shaped elastic thin-wall boom, a tubular airbag, and a Velcro. The tubular airbag has a transverse diameter of 10 cm, a thickness of 10μm, and a longitudinal length of 1.3 m. The Velcro has a thickness of 3 mm and a lateral width of 15 mm. The rigid roller acts as an auxiliary crimping tool with a diameter of 250 mm and a mass of 1.88 kg. The finite element model of the initial state without stress is shown in Figure 21. In this model, the tubular cavity is located in the middle of the elastic thin-walled rod, and the central line of the bottom surface of the cavity is fixed to the thin-walled rod. The Velcro is located on a straight section on both sides of the thin-walled rod, and the lower base surface is fixed to the thin-walled rod.

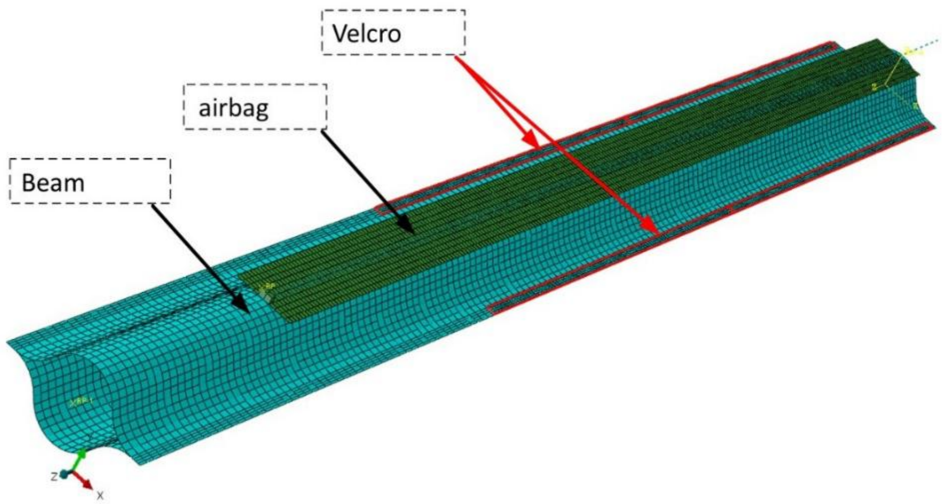

Figure 21: The finite element model of inflated deployment boom

(1) The rolling process of the structure

The curled state is the initial configuration of the elastic thin-wall boom. In the state without external force, the sectional configuration of the thin-wall boom is as shown in Figure 22, and the geometric shape is symmetrical. How to obtain the curled configuration from the initial state is the key to the analysis of the thin-wall boom's deployment process. In order to solve this problem, the boom end portion is pre-treated by first pulling and re-crimping to ensure that the upper and lower thin walls of the boom are closely attached to the roller.
The first step is the tension and compression process. Two sections are taken as the tension application area at the flat ends on both sides of the boom end. In order to avoid excessive deformation of the thin-wall boom elements by the tensile force, the mesh density of this area is increased.

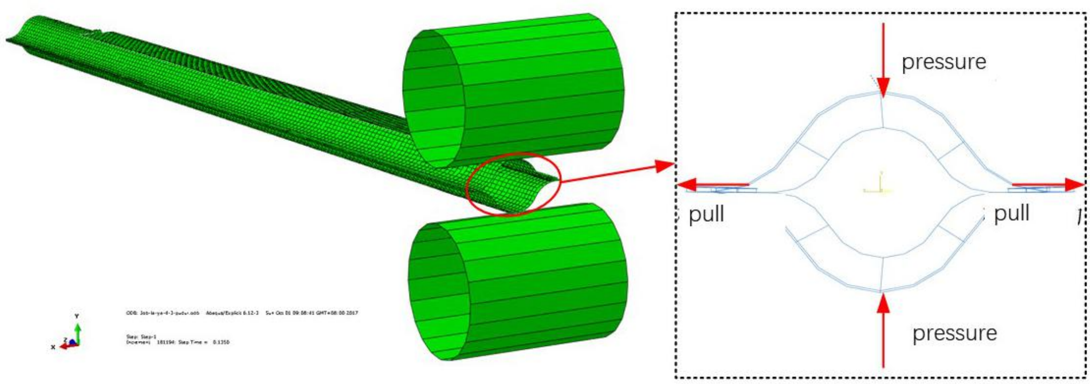

Figure 22: The sectional configuration of the thin-wall boom

DOI: 10.13009/EUCASS2019-86

Before the curling action, the TIE method should be fixed between the edge of the upper and lower boom wall of the thin-wall boom end and the outer surface of the roller. Because the constraint mode TIE is defined at the beginning of the model analysis, two analysis models need to be established, each of which The geometric parameters of the components, the grid size is exactly the same, one of which is the tension and compression model, and the other is the curly model. Then use the load module of ABAQUS to define the initial state of the curling model, and then transfer the final stress and deformation state of the tensioning model to the crimping model to complete the preparation before crimping. Finally ,we get the model as shown in Figure 23.

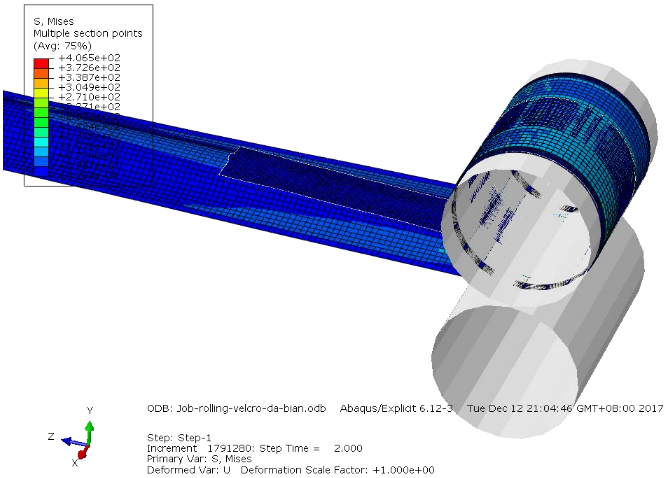

Figure 23: The model of boom after rolling

(2) The process of inflation deployment

The tubular airbag in the above model was inflated, the inflation flow rate was 3.24 kg/h, and the inflation time was 1.6s.As shown in Fig24, the airbag at the initial moment of inflation is in a flat state, and there is no obvious force between it and the thin-walled rod. As the airbag continues to bulge during inflation, thrust is generated on the wall of the boom in contact, and when the force is increased enough to overcome the Velcro's binding force, the thin-wall boom begins to expand and deploy.

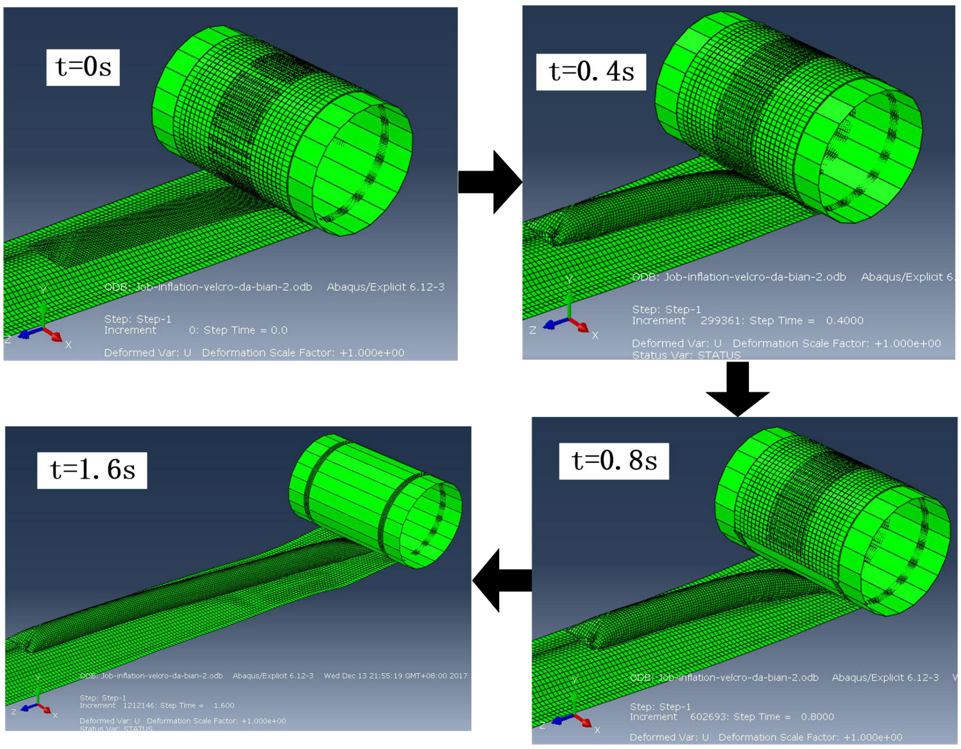

Figure 24: The process of deployment of infalted boom

DOI: 10.13009/EUCASS2019-86

Figure25 shows the variation of the internal pressure and deployment displacement of the airbag during the deployment process from the inflation simulation model.

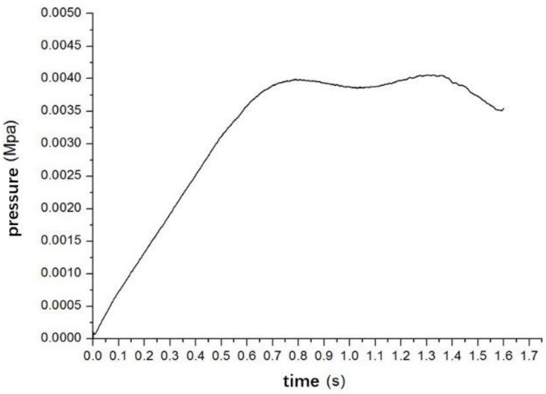

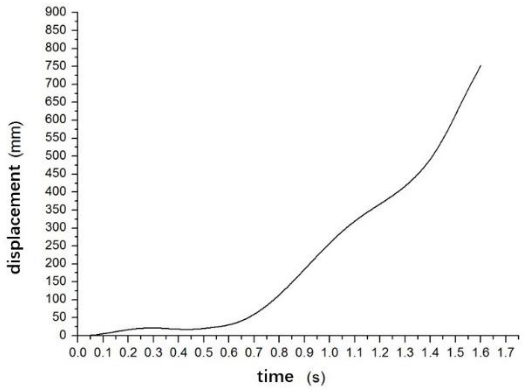

Figure 25: The airbag internal pressure curve(left) and displacement curve(right)

It can be seen from the curves in Fig 25 (lest) that when the inflation starts, the pressure in the airbag gradually rises, and the roller at this time does not immediately move due to the binding force of the Velcro. When t=0.6s, the airbag pressure is increased to about 0.004 MPa, at which point the Velcro begins to be peeled and the deployment begins. It can be seen from the pressure change curves that the internal pressure of the airbag during deployment is slowly changed within a small range, which provides a relatively stable driving force for the deployment motion.

4. Conclusion

Based on the CFRP boom, the Velcro and the airbag, a inflated deployment boom constrained by Velcro is designed, and the dynamic characteristics of the structure are carried out. The main research results include: (1) designing the elastic thin-wall boom inflated structure and establishing its finite element model; (2) by designing the simulation parameters, the simulation of the inflating process of a single elastic thin-walled rod is realized;

The innovations in this paper include:1. The equivalent finite element model of the Velcro process is established, and the relevant experimental verification is completed. Compared with methods such as stress failure beam, this method has significant advantages in high modelling efficiency and fast calculation speed. The simulation analysis model of large deformation structure under the coupling of airbag driving force, gluing binding force and thin wall rod elastic restoring force is established.

It can be seen from the above research results that the research on the inflation deployment process under the elastic state of the elastic thin-wall boom has gone through the research process from the sub-component to the overall structure. This process is not only a process of deepening the understanding of the relevant characteristics of Velcro , airbags, and CFRP boom , but also lays a good foundation for further research.

References

[1] Herbeck L, Leipold M, Sickinger C, et al. Development and test of deployable ultra-lightweight cfrp-booms for a solar sail[C]//Spacecraft Structures, Materials and Mechanical Testing. 2001, 468: 107.
[2] Straubel M, Block J, Sinapius M, et al. Deployable composite booms for various gossamer space structures[C]//52nd AIAA/asme/asce/ahs/asc Structures, Structural Dynamics, and Materials Conference. 2011.
[3] Chen W, Fang G, Hu Y. An experimental and numerical study of flattening and wrapping process of deployable composite thin-walled lenticular tubes[J]. Thin-Walled Structures, 2017, 111: 38-47.
[4] Fang H, Lou M, Hah J. Deployment study of a self-rigidizable inflatable boom[J]. Journal of spacecraft and rockets, 2006, 43(1): 25-30.
[5] Salama M, Fang H, Lou M. Resistive deployment of inflatable structures using Velcro[J]. Journal of spacecraft and rockets, 2002, 39(5): 711-716.
[6] Perez V R. Multiscale strategy for modelling the mechanical performance of hook and loop fasteners based on a detachment process zone model[D]. Purdue University, 2016.
[7] Wong J C. Modeling of High Pressure Confined Inflatable Structures[M]. West Virginia University, 2013.